

# DIELECTRIC PROPERTIES OF FeGaInS<sub>4</sub>/PVA COMPOSITES: INFLUENCE OF FILLER CONCENTRATIONS

## VPLIV KONCENTRACIJE POLNILA NA DIELEKTRIČNE LASTNOSTI KOMPOZITOV FeGaInS<sub>4</sub>/PVA

**Mahammad Baghir Baghirov<sup>1</sup>, Mustafa Muradov<sup>1</sup>, Zeynab Addayeva<sup>1</sup>,  
Namiq Niftiyev<sup>2</sup>, Faik Mammadov<sup>2,3</sup>, Goncha Eyvazova<sup>1</sup>, Marjetka Conradi<sup>4\*</sup>**

<sup>1</sup>Nano Research Laboratory, Baku State University, 23 Academic Zahid Khalilov Street, Baku, AZ1148, Azerbaijan

<sup>2</sup>Azerbaijan State Pedagogical University, Az-1000, Baku, Azerbaijan

<sup>3</sup>Institute of Catalysis and Inorganic Chemistry, AZ-1143, Baku, Azerbaijan

<sup>4</sup>Institute of Metals and Technology, Lepi pot 11, 1000, Ljubljana, Slovenia

*Prejem rokopisa – received: 2025-04-25; sprejem za objavo – accepted for publication: 2025-06-23*

doi:10.17222/mit.2025.1445

Dielectric permittivity is a crucial factor in the development of advanced electronic components, with its control achieved by varying filler concentrations. This study explores the dielectric properties – permittivity ( $\epsilon'$ ), dielectric loss tangent ( $\tan \delta$ ), and electrical conductivity ( $\sigma$ ) – of PVA composites containing 1 w%, 3 w%, and 5 w% FeGaInS<sub>4</sub> crystals over a frequency range of 120 Hz to 1 MHz at 293 K. A structural analysis was performed using X-ray diffraction (XRD), and the filler morphology and crystallite size were examined with transmission electron microscopy (TEM). Results revealed a decrease in  $\epsilon'$  with increasing frequency, primarily due to interfacial polarization at low frequencies. The addition of 1 w% FeGaInS<sub>4</sub> enhanced  $\epsilon'$  due to interfacial layer formation and Maxwell–Wagner–Sillars (MWS) polarization. Conversely, higher concentrations (3 w% and 5 w%) caused a decline in  $\epsilon'$ , attributed to filler agglomeration and diminished interfacial effects. A dielectric loss analysis indicated relaxation processes tied to changes in conductivity induced by localized charge carriers. Key electrical parameters at 293 K and 1 kHz included a consistent potential barrier height ( $W_M = 2.16$  eV), hopping distance ( $R_w = 5.36 \times 10^{-10}$  m to  $11.3 \times 10^{-10}$  m), and density of localized states ( $N = 11 \times 10^{27}$  m<sup>-3</sup> to  $1.07 \times 10^{27}$  m<sup>-3</sup>). A mixed-zone and hopping conduction mechanism was identified. These findings highlight the role of filler concentration in tailoring the dielectric properties for advanced applications.

**Keywords:** FeInGaS<sub>4</sub>/PVA composites, dielectric properties, electrical conductivity, semiconductor filler.

Dielektrična permitivnost je ključni dejavnik pri razvoju naprednih elektronskih komponent, pri čemer njeno uravnavanje dosežemo s spreminjanjem koncentracije polnila. Ta študija raziskuje dielektrične lastnosti – permitivnost ( $\epsilon'$ ), dielektrični tangent izgub ( $\tan \delta$ ) in električno prevodnost ( $\sigma$ ) – PVA kompozitov, ki vsebujejo 1 w%, 3 w% in 5 w% kristalov FeGaInS<sub>4</sub>, v frekvenčnem območju od 120 Hz do 1 MHz pri 293 K. Strukturna analiza je bila izvedena z uporabo rentgenske difrakcije (XRD), morfologija polnila in velikost kristalitov pa sta bili preučeni s pomočjo presečne elektronske mikroskopije (TEM). Rezultati so pokazali zmanjšanje  $\epsilon'$  z naraščajočo frekvenco, kar je predvsem posledica medfazne polarizacije pri nizkih frekvencah. Dodatek 1 w% FeGaInS<sub>4</sub> je povečal  $\epsilon'$  zaradi nastanka medfaznih plasti in Maxwell–Wagner–Sillarsove (MWS) polarizacije. Nasprotno pa so višje koncentracije (3 w% in 5 w%) povzročile zmanjšanje  $\epsilon'$ , kar pripisujemo aglomeraciji polnila in zmanjšanim medfaznim učinkom. Analiza dielektričnih izgub je pokazala relaksacijske procese, povezane s spremembami v prevodnosti, ki jih povzročajo lokalizirani nosilci naboja. Ključni električni parametri pri 293 K in 1 kHz so vključevali dosledno višino potencialne bariere ( $W_M = 2.16$  eV), skakalno razdaljo ( $R_w = 5.36 \times 10^{-10}$  m do  $11.3 \times 10^{-10}$  m) in gostoto lokaliziranih stanj ( $N = 11 \times 10^{27}$  m<sup>-3</sup> do  $1.07 \times 10^{27}$  m<sup>-3</sup>). Identificiran je bil mehanizem prevodnosti, ki vključuje mešano območje in skakanje nosilcev naboja. Ti rezultati poudarjajo vlogo koncentracije polnila pri prilagajanju dielektričnih lastnosti za napredne aplikacije.

**Ključne besede:** FeInGaS<sub>4</sub>/PVA kompoziti, dielektrične lastnosti, električna prevodnost, polprevodniški vključki

## 1 INTRODUCTION

2D structures not only form the foundation of modern electronics but also hold significant potential for future advances due to their tunable properties.<sup>1</sup> These layered crystals consist of sheets bonded strongly through covalent or ionic interactions in the horizontal plane and much weaker van der Waals interactions in the vertical direction, which stack to form layered structures.<sup>2</sup> By utilizing the low energy of van der Waals interactions in

layered crystals synthesized with various methods, it is possible to control their bandgap by reducing the number of layers.<sup>3</sup> Additionally, surface defects and dangling bonds formed by unbound electrons can be eliminated when layers are stacked, leading to the development of more stable materials. These structures, also referred to as van der Waals crystals, exhibit unique properties due to their high surface-to-volume ratio.<sup>4</sup> The activation of surface area and other characteristics at smaller dimensions significantly expands their application range.<sup>5</sup>

Recently, polymers and polymer composites, which aim to enhance polymer properties, have become widely used in both industry and research. Polymer composites are created by incorporating various fillers into a poly-

\*Corresponding author's e-mail:  
marjetka.conradi@imt.si (Marjetka Conradi)



© 2025 The Author(s). Except when otherwise noted, articles in this journal are published under the terms and conditions of the Creative Commons Attribution 4.0 International License (CC BY 4.0).

mer matrix.<sup>6</sup> Although polymer composites prepared using 2D structures as fillers are particularly intriguing, they remain less explored compared to other composites. Layered 2D structures, with their unique properties, stand out in polymer composites.<sup>7</sup> The small size of these fillers leads to surface and quantum effects, creating an interfacial layer at the boundary between the filler and the polymer. This interfacial layer, formed through interactions between the polymer and filler, significantly impacts the composite's properties, which can differ substantially from those of the polymer or the filler alone.<sup>8</sup> Furthermore, the large surface area of 2D fillers and the ability of the polymer to penetrate between the weakly bonded layers of van der Waals crystals enhance the interfacial layer, thereby altering the composite's properties.<sup>9</sup>

One of the characteristics influenced by the interfacial layer is polarization, along with conductivity.<sup>10</sup> According to the Lewis theoretical model, when free charges accumulate on the surface of an active particle, the negative charges of the polymer distribute densely along the surface, forming a dipole-like structure.<sup>11</sup> Based on the double electron layer model, a dense region of charges near the surface forms the Stern layer, while a more flexible field of charges farther away constitutes the diffuse layer.<sup>12</sup> Polarization within these layers, driven by Maxwell–Wagner–Sillars (MWS) interfacial polarization, alters the composite's dielectric properties. The properties and concentration of the fillers also affect the composite's electrical characteristics.<sup>13</sup> At low concentrations, the large distances between well-dispersed particles result in minimal interactions among interfacial zones. However, as the filler concentration increases, in-

teractions, as well as agglomeration and percolation effects, significantly alter the composite's electrical conductivity.<sup>14</sup> Therefore, understanding how the concentration of crystals influences the electrical properties of polymers is crucial.

In this study, FeGaInS<sub>4</sub> crystals, which have been explored to a limited extent, were employed. These crystals were initially synthesized during investigations of the FeGa<sub>2</sub>S<sub>4</sub>-FeIn<sub>2</sub>S<sub>4</sub> system. The structure of FeGaInS<sub>4</sub> has been characterized and exhibits a trigonal configuration.<sup>16–18</sup> The lattice parameters are  $a = 0.37765(1)$  nm and  $c = 1.22257(3)$  nm, with an activation energy of  $\Delta E = 0.21$  eV.<sup>19–21</sup> Despite the semiconductor properties of these layered crystals, their integration into polymer matrices as composites has been minimally investigated.<sup>22</sup> In this study, polyvinyl alcohol (PVA) was used as the polymer matrix. The research examines the structure and dimensions of FeGaInS<sub>4</sub> crystals and the changes in dielectric properties of PVA-based composites with varying filler concentrations. Thin films of PVA mixed with FeGaInS<sub>4</sub> crystals at 1 w/%, 3 w/%, and 5 w/% concentrations were analyzed. The composite structures were characterized using X-ray diffraction (XRD), while dielectric properties were measured using dielectric spectroscopy. The morphology (shape and size) of the crystals were determined by transmission electron microscopy (TEM).

## 2 MATERIALS AND METHODS

The structural analysis of FeGaInS<sub>4</sub>/PVA composites was conducted using a Rigaku Mini Flex 600 X-ray diffractometer with Ni-filtered Cu-K $\alpha$  radiation

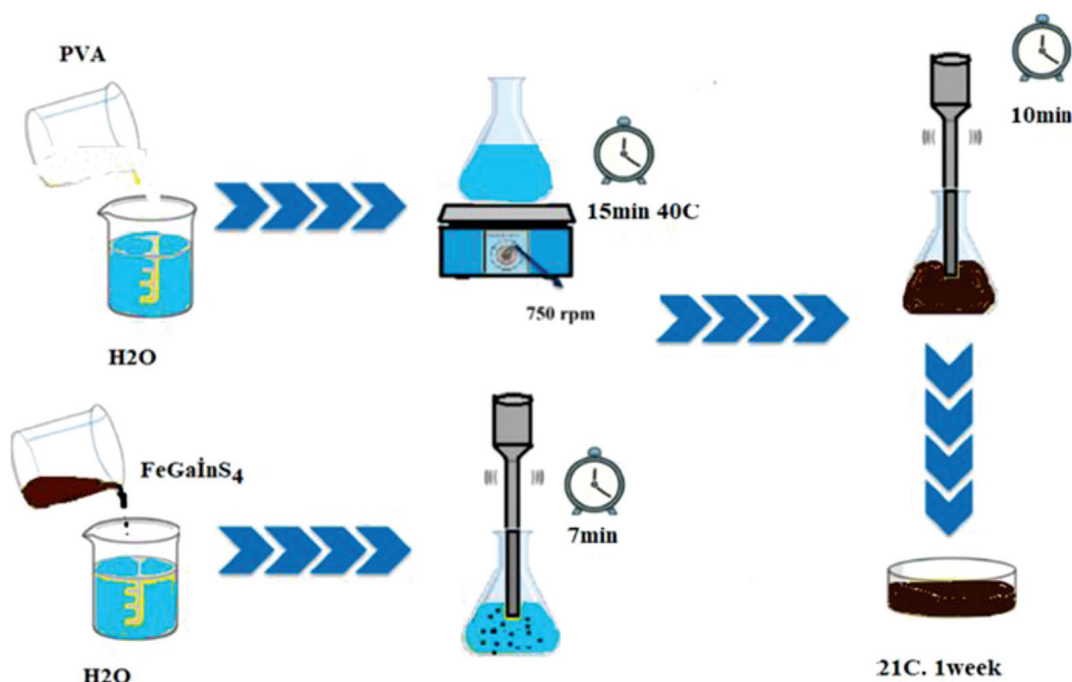


**Figure 1:** Synthesis of PVA based composites

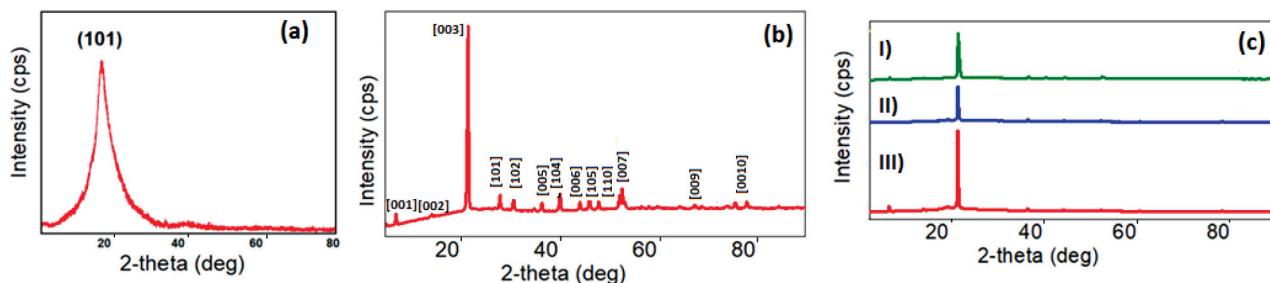


**Figure 2:** X-ray diffraction patterns of (I) FeGaInS<sub>4</sub> crystals and (II) the surface layer of PVA+FeGaInS<sub>4</sub> composites: a) 1 % FeGaInS<sub>4</sub>+PVA, b) 3 % FeGaInS<sub>4</sub>+PVA, c) 5 % FeGaInS<sub>4</sub>+PVA

( $\lambda = 0.15406$  nm). Transmission Electron Microscopy (TEM) was performed using a JEM-1400 (JEOL, Japan) at 80–120 kV. Morphometric analysis of the electronograms was conducted in TIF format using the TEM Imaging Platform-ITEM software (Olympus Soft Imaging Solutions GmbH, Germany). The electrical properties were measured using an E7-20 dielectric spectrometer.

FeGaInS<sub>4</sub> crystals were synthesized by mixing FeGa<sub>2</sub>S<sub>4</sub> and FeIn<sub>2</sub>S<sub>4</sub> compounds in a 1:1 molar ratio. The stoichiometric mixture was sealed in an evacuated quartz ampoule and placed in a two-zone furnace for crystal growth. To enhance the crystallinity of the synthesized samples, they were thermally treated at 800 K for 100 h.<sup>18,20,21</sup>

As described in the study, the synthesized crystal powder was incorporated into a polyvinyl alcohol (PVA) polymer matrix. For this purpose, a solution of PVA in distilled water was prepared. The crystals were mechanically ground, and FeGaInS<sub>4</sub> crystals at weight concentrations of 1 w/%, 3 w/%, and 5 w/% were added to the PVA solution. Each solution was subjected to ultrasonic treatment for 4 min. The resulting solutions were filtered into Petri dishes and left to dry at room temperature.<sup>22</sup> The obtained films were analyzed for structural determination using X-ray diffraction and for dielectric property measurements. The synthesis process is shown in **Figure 1**.

### 3 RESULT AND DISCUSSION

#### 3.1 X-ray analysis

X-ray diffraction (XRD) analysis was performed to investigate the crystalline structure of the FeGaInS<sub>4</sub> crystal and the FeGaInS<sub>4</sub>/PVA composites synthesized at room temperature. **Figure 1a** shows the X-ray diffraction pattern of pure PVA, while **Figure 1b** displays the diffraction pattern of the FeGaInS<sub>4</sub> crystal. The diffraction patterns of the composite samples containing different concentrations of FeGaInS<sub>4</sub> – specifically 1 w/%, 3 w/%, and 5 w/% – are presented in **Figure 2c** and labeled as I, II, and III, respectively.

The diffraction peaks observed at  $2\theta$  values of  $8.1^\circ$ ,  $14.64^\circ$ ,  $21.8^\circ$ ,  $37^\circ$ ,  $40.8^\circ$ ,  $44.3^\circ$ ,  $46.67^\circ$ ,  $48.1^\circ$ ,  $52.63^\circ$ ,  $69.3^\circ$  and  $78.6^\circ$  correspond to the (001), (002), (003),

(101), (102), (005), (104), (006), (105), (110) (007), (009), and (0010) planes of FeGaInS<sub>4</sub> crystals.<sup>16</sup> The consistency of these peaks confirms that the crystal structure of the FeGaInS<sub>4</sub> remains unchanged upon composite formation. Additionally, the prominent peak at  $2\theta = 19.31^\circ$  is attributed to the characteristic diffraction of PVA.<sup>23–25</sup>

#### 3.2 TEM images of FeGaInS<sub>4</sub>

The determination of the particle sizes after ultrasonic dispersion was performed using TEM. The TEM images of the fragmented crystals are shown in **Figure 3**. The images clearly reveal the layered structure of the crystals. TEM analysis revealed that the particles predominantly exhibited sizes around 490 nm and 790 nm; however, smaller crystallites, including those in the range of  $\approx 20$  nm, were also observed, albeit in much lower abundance.

#### 3.3 Dielectric properties analysis

The dielectric properties of polymer composites prepared at various concentrations were studied using a dielectric spectrometer at room temperature under different conditions.

**Figure 4** presents the dependence of the real part of the relative dielectric permittivity ( $\epsilon'$ ) on the frequency of the alternating electric field for pure PVA and composites with 1 w/%, 3 w/%, and 5 w/% FeGaInS<sub>4</sub> at room temperature. Within the investigated frequency range, the values  $\epsilon'$  vary between approximately 5 and 10.

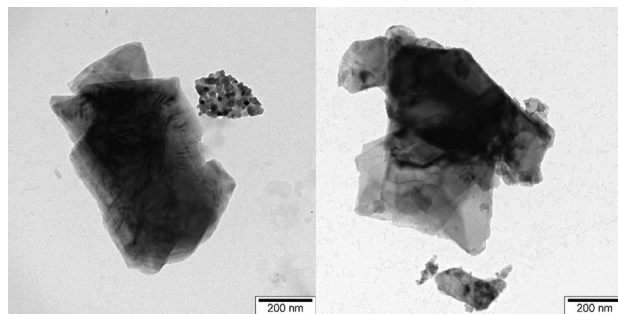


**Figure 3:** TEM images of FeGaInS<sub>4</sub> crystals

The graph shows that for all samples,  $\epsilon'$  decreases as the frequency increases in the range of  $1.2 \cdot 10^2$ – $10^5$  Hz. This reduction is attributed to interphase polarization, which becomes significant at lower frequencies. As the frequency increases, the dipoles cannot align with the field. Initially, dipoles with lower relaxation rates align with the field, but with further increases in frequency, the number of dipoles unable to align increases. At low frequencies, the electric field changes direction slowly enough that dipoles (molecular or ionic entities with an electric moment) have sufficient time to reorient themselves in the direction of the field. Dipoles with lower relaxation rates (i.e., slower response times) can still follow these slower field changes.

However, as the frequency of the electric field increases, the direction of the field starts changing much faster. At a certain point, some dipoles can no longer keep up – their natural relaxation time is too slow compared to the oscillation of the field. These dipoles fail to reorient in time, and thus do not contribute effectively to the polarization.

This is why the effective dielectric constant  $\epsilon'$  stops increasing or even decreases at higher frequencies – fewer dipoles are able to align with the rapidly alternating field, reducing the overall polarization of the material.

This phenomenon is known as dielectric dispersion, and it is typically explained by models like the Debye relaxation model.

In the frequency range of  $10^5$  to  $5 \cdot 10^5$  Hz,  $\epsilon'$  remains almost constant. However, in the frequency range  $5 \cdot 10^5$  Hz to  $10^6$  Hz, an increase in  $\epsilon'$  with frequency is observed.<sup>22</sup>

The data indicate that the addition of FeGaInS<sub>4</sub> crystals to PVA increases the real part of the dielectric

permittivity at 1 w/% concentration. However, a decrease in  $\epsilon'$  is observed for samples with 3 w/% and 5 w/% crystal content. The increase in  $\epsilon'$  at 1 w/% concentration is attributed to the formation of an interphase layer on the crystal surfaces within the polymer matrix, which enhances the Maxwell–Wagner–Sillars (MWS) polarization. In contrast, at higher concentrations (3 w/% and 5 w/%), agglomeration of the filler particles and the growth in crystal size hinder the mobility of the functional groups of the polymer under the influence of the electric field, thereby reducing the free volume of the polymer and, consequently, the dielectric permittivity of the composite.

**Figure 5** depicts the frequency dependence of the dielectric loss tangent ( $\tan \delta$ ) for pure PVA and FeGaInS<sub>4</sub>/PVA composites with concentrations of 1 w/%, 3 w/%, and 5 w/% at room temperature (293 K). The results show that in the frequency range of  $1.2 \cdot 10^2$  to  $5 \cdot 10^2$  Hz,  $\tan \delta$  decreases with increasing frequency for all samples. In the intermediate frequency range of  $10^3$  Hz to  $5 \cdot 10^4$  Hz,  $\tan \delta$  remains nearly constant across all samples. However, at higher frequencies,  $5 \cdot 10^4$  to  $10^6$ , maximum in  $\tan \delta$  is observed.

These observed maxima in the frequency dependence of the dielectric loss are associated with the relaxation processes of charge carriers. The decrease in  $\tan \delta$  at low frequencies can be attributed to the alignment of dipoles, while the nearly constant behavior in the intermediate frequency range suggests stabilized dielectric loss. The increase at higher frequencies reflects the contribution of charge-carrier relaxation phenomena within the composites.

As shown in **Figure 5**, the dielectric loss undergoes significant changes with the incorporation of semiconductor crystallites into the polymer matrix. This variation is primarily due to the modification in the material's conductivity, driven by the addition of crystallites into polymers with localized charge carriers. The dependence of the dielectric loss on the frequency of the applied electric

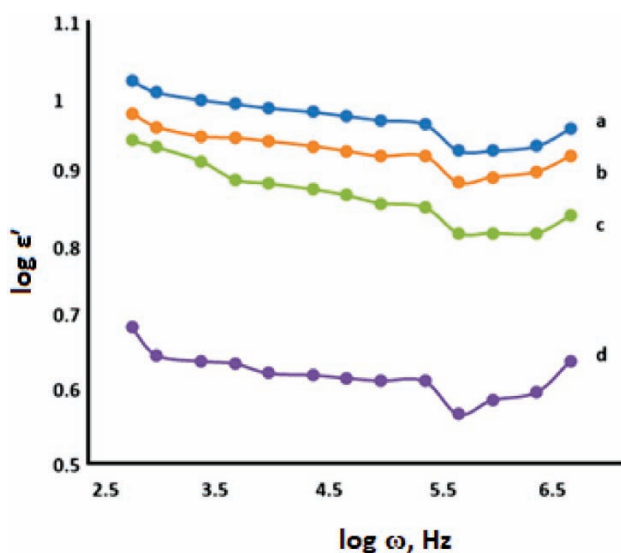


**Figure 4:** a) 1 w/% FeGaInS<sub>4</sub>/PVA, b) pure PVA, c) 3 w/% FeGaInS<sub>4</sub>/PVA, and d) 5 w/% FeGaInS<sub>4</sub>/PVA, showing the relationship between  $\epsilon'$  and the electric field frequency

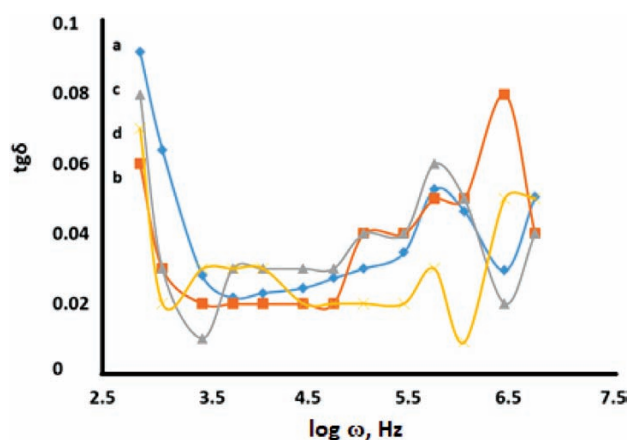


**Figure 5:** Dependence of dielectric loss angle tangent on electric field frequency at 293 K for a) pure PVA, b) 1 w/% FeGaInS<sub>4</sub>/PVA, c) 1 w/% FeGaInS<sub>4</sub>/PVA, d) 1 w/% FeGaInS<sub>4</sub>/PVA



field is inherently tied to the conduction mechanism of the material. Specifically, the frequency dependence of the electrical conductivity can alter the dielectric loss behavior. In many materials, this relationship is characterized by the empirical power law  $\sigma \approx \omega^s$ , where  $0.1 \leq s \leq 1.0$ , which is indicative of a hopping conduction mechanism.<sup>26</sup> Considering what has been said, the frequency dependence of the dielectric loss angle tangent for various mechanisms that play a dominant role in conductivity can be expressed as follows:

$$\operatorname{tg} \delta(\omega) \approx \omega(\omega^{-1} + \omega) \text{ Band mechanism} \quad (1)$$

$$\operatorname{tg} \delta(\omega) \approx \omega(\omega^{s-2} + 1) \text{ Hopping mechanism} \quad (2)$$

Equation (1) indicates that a linear dependence of the function  $\operatorname{tg} \delta(\omega) = f(\omega)$  should be observed in the band mechanism, which plays a dominant role in conductivity.

**Figure 6** presents the dependence of  $\ln(\operatorname{tg} \delta(\omega))$  on  $\ln(\omega)$  at room temperature (293K) for pure PVA and the 1 w/%, 3 w/%, and 5 w/% FeGaInS<sub>4</sub>/PVA composite samples. The figure reveals that the resulting curves are approximately linear over a certain frequency range but deviate from perfect linearity outside this region. This behavior indicates that the electrical conductivity in these samples arises from a combination of band-like (zone) conduction and hopping conduction mechanisms. The linear segments suggest band conduction in extended states, while deviations from linearity imply contributions from hopping mechanisms, where localized charge carriers dominate conductivity in specific frequency regimes.

**Figure 7** depicts the frequency dependence of electrical conductivity for pure PVA and FeGaInS<sub>4</sub>-based composites with 1 w/%, 3 w/%, and 5 w/% concentrations, measured at room temperature. As observed, the introduction of FeGaInS<sub>4</sub> filler into the PVA matrix enhances the electrical conductivity up to a concentration of 3 w/%, beyond which, in the 5 w/% sample, a decrease in  $\sigma$  is noted. The graph further indicates that electrical conductivity increases with rising frequency in the range of  $1.2 \cdot 10^2$  Hz to  $2 \cdot 10^5$  Hz for all studied samples.

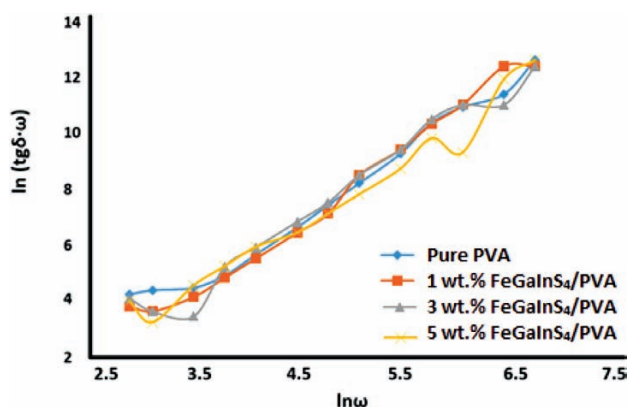


**Figure 6:**  $\ln(\operatorname{tg} \delta \cdot \omega) \approx \ln \omega$  dependence at 293 K for pure PVA, 1 %, 3 % and 5 % FeGaInS<sub>4</sub>-based composites

In this frequency range, the conductivity follows the power law

$$\sigma \approx \omega^s \quad (3)$$

indicating a direct relationship between frequency and conductivity. For these composites, the exponent  $s$  varies between 0.10 and 1.32, depending on the frequency in the range  $1.2 \cdot 10^2$  Hz to  $10^5$  Hz at room temperature (293K). This variation in  $s$  suggests different conduction mechanisms, potentially involving both band-like and hopping conduction processes, depending on the filler concentration and frequency.

One of the most prominent models describing charge transport in polymeric materials is the Correlated Barrier Hopping (CBH) model, which involves electron hopping through potential barriers.<sup>27</sup> According to the CBH model, electrons overcome potential barriers and jump between energy states.<sup>27–29</sup> The expression for the conductivity in an alternating electric field as per the CBH model is given by:

$$\sigma(\omega) = \frac{\pi^3 N^2 \varepsilon \varepsilon_0 \omega R_\omega^6}{24} \quad (4)$$

Here,  $N$  is the density of pairs of states between which the charge carriers hop,  $\varepsilon$  is the dielectric constant of the medium,  $\varepsilon_0$  is the permittivity of free space,  $\omega$  is the angular frequency, and  $R_\omega$  is the hopping length.

The relationship between the hopping length  $R_\omega$  and the height of the potential barrier  $W_M$  is expressed as:

$$R_\omega = \frac{e^2}{\pi \varepsilon \varepsilon_0} \left[ W_M - kT \ln \left( \frac{1}{\omega \tau_0} \right) \right]^{-1} \quad (5)$$

In this expression,  $\tau_0$  represents the characteristic relaxation time, which is the inverse of the phonon frequency  $\nu_f$  and  $k$  is the Boltzmann constant. The parameter  $W_M$  denotes the height of the potential barrier.

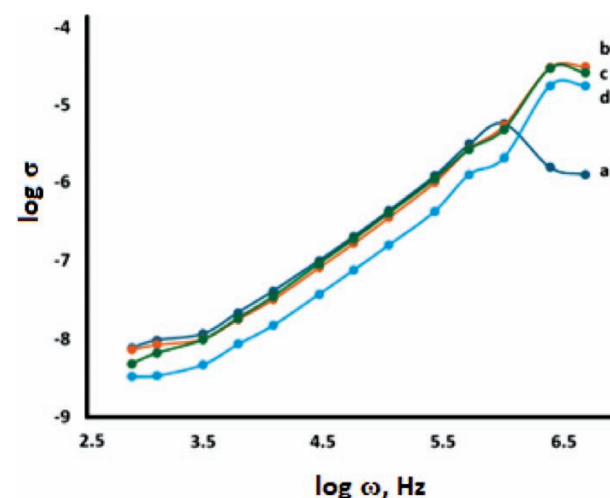


**Figure 7:** Dependence of electrical conductivity on the frequency of the applied electric field at 293 K for FeGaInS<sub>4</sub>-based composites with a) pure PVA, b) 1 w/% FeGaInS<sub>4</sub>/PVA, c) 1 w/% FeGaInS<sub>4</sub>/PVA, d) 1 w/% FeGaInS<sub>4</sub>/PVA

The exponent  $s$ , which characterizes the frequency dependence of conductivity, is related to the potential barrier height  $W_M$  by the following relation:

$$s = 1 - \frac{6kT}{[W_M - kT / (\omega\tau_0)]} \quad (6)$$

To simplify, in the first approximation,  $s$  can be expressed as:

$$s = 1 - \frac{6kT}{W_M} \quad (7)$$

Using the experimental data obtained, the parameters of the systems were calculated at a temperature of 293 K and a frequency of 10<sup>3</sup> Hz for pure PVA and the 1 w/%, 3 w/%, and 5 w/% FeGaInS<sub>4</sub>-based composites. The calculated values for these parameters are presented in **Table 1**.

**Table 1:** The calculated values of the hopping length ( $R_\omega$ ), density of localized state pairs ( $N$ ), and potential barrier height ( $W_M$ )

Samples	$R_\omega$ , m ( $\times 10^{-10}$ )	$N$ , m <sup>-3</sup> ( $\times 10^{27}$ )	$W_M$ , eV
pure PVA	5.36	11.0	2.16
FeGaInS <sub>4</sub> /PVA (1 w/%)	6.12	7.17	2.16
FeGaInS <sub>4</sub> /PVA (3 w/%)	6.48	6.3	2.16
FeGaInS <sub>4</sub> /PVA (5 w/%)	11.30	1.07	2.16

#### 4 CONCLUSIONS

In this study, FeGaInS<sub>4</sub>/PVA composites with varying concentrations (1 w/%, 3 w/%, and 5 w/%) were synthesized using a mechanical mixing technique. The structural, morphological, and dielectric properties of the resulting samples were systematically investigated. X-ray diffraction (XRD) analysis confirmed that the incorporation of FeGaInS<sub>4</sub> did not induce any structural changes in the composites across all concentrations. Transmission electron microscopy (TEM) revealed that while the majority of crystallites ranged in size between approximately 490 nm and 790 nm, smaller crystallites were also observed in lower quantities.

Dielectric property analysis showed that the dielectric permittivity ( $\epsilon'$ ) decreased with increasing frequency, within the range of  $1.2 \times 10^2$  to  $5 \times 10^5$  Hz, for all samples – a behavior attributed to interfacial polarization, which is more pronounced at lower frequencies. Interestingly, at a 1 w/% FeGaInS<sub>4</sub> concentration, an enhancement in the dielectric permittivity of the polymer was observed, whereas further increases to 3 w/% and 5 w/% resulted in a decline in  $\epsilon'$ , attributed to mechanisms discussed in the text.

The incorporation of FeGaInS<sub>4</sub> crystallites also affected the dielectric loss behavior, linked to changes in electrical conductivity. The maximum observed in the frequency dependence of dielectric loss is associated with charge carrier relaxation processes. Using the correlated barrier hopping (CBH) model, system parameters were evaluated for the composites at 293 K and a fre-

quency of 10<sup>3</sup> Hz. The analysis revealed consistent results across all concentrations, with a potential barrier height ( $W_M$ ) of 2.16 eV and hopping distances ( $R_\omega$ ) ranging from  $5.36 \times 10^{-10}$  m to  $11.30 \times 10^{-10}$  m.

These findings suggest that electrical conduction in the FeGaInS<sub>4</sub>/PVA composites is governed by a combination of band-like and hopping conduction mechanisms. Furthermore, the relative concentration of the semiconductor phase in the polymer matrix can be effectively tuned to modulate the electrical conductivity of the composites.

#### Funding

The authors acknowledge the financial support from the Slovenian Research Agency (research core funding No. P2-0132).

#### 5 REFERENCE

- P. Kaushal, G. Khanna, The role of 2-Dimensional materials for electronic devices, *Materials Science in Semiconductor Processing*, 143 (2022), 106546, doi:10.1016/j.mssp.2022.106546
- R. M. A. Lieth (Ed.), *Preparation and Crystal Growth of Materials with Layered Structures*, vol. 1, Springer, 1977, doi:10.1007/978-94-017-2750-1
- A. Chaves, et al., Bandgap engineering of two-dimensional semiconductor materials, *npj 2D Materials and Applications*, 4 (2020), 29, doi:10.1038/s41699-020-00162-4
- K. S. Novoselov, et al., 2D materials and van der Waals heterostructures, *Science*, 353 (2016), aac9439, doi:10.1126/science.aac9439
- K. Choi, Y. T. Lee, S. Im, Two-dimensional van der Waals nanosheet devices for future electronics and photonics, *Nano Today*, 11 (2016), 5, 626–643, doi:10.1016/j.nantod.2016.08.007
- K. I. Winey, R. A. Vaia, Polymer nanocomposites, *MRS Bulletin*, 32 (2007), 4, 314–322, doi:10.1557/mrs2007.217
- A. Ali, et al., Materials innovations in 2D-filler reinforced dielectric polymer composites, *Materials Innovation*, 2 (2022), 47–66, doi:10.54738/MI.2022.2202
- M. G. Todd, F. G. Shi, Characterizing the interphase dielectric constant of polymer composite materials: effect of chemical coupling agents, *Journal of Applied Physics*, 94 (2003), 7, 4551–4557, doi:10.1063/1.1604961
- J. Seiler, J. Kindersberger, Insight into the interphase in polymer nanocomposites, *IEEE Transactions on Dielectrics and Electrical Insulation*, 21 (2014), 2, 537–547, doi:10.1088/1757-899X/1116/1/012023
- P. Gupta, et al., Dielectric properties of polymer nanocomposite interphases using electrostatic force microscopy and machine learning, *ACS Applied Electronic Materials*, 5 (2023), 2, 794–802, doi:10.1021/acsaem.2c01331
- J. Huang, J. Zhou, M. Liu, Interphase in polymer nanocomposites, *JACS Au*, 2 (2022), 2, 280–291, doi:10.1021/jacsau.1c00430
- H. Hu, et al., Recent advances in rational design of polymer nanocomposite dielectrics for energy storage, *Nano Energy*, 74 (2020), 104844, doi:10.1016/j.nanoen.2020.104844
- E. Tuncer, et al., Enhancement of dielectric strength in nanocomposites, *Nanotechnology*, 18 (2007), 32, 325704, doi:10.1088/0957-4484/18/32/325704
- M. I. Mohammed, Dielectric dispersion and relaxations in (PMMA/PVDF)/ZnO nanocomposites, *Polymer Bulletin*, 79 (2022), 4, 2443–2459, doi:10.1007/s00289-021-03606-z

- <sup>15</sup> Z. Ahmad, Polymer dielectric materials, in: *Dielectric Material*, IntechOpen, 2012, doi:10.5772/50638
- <sup>16</sup> F. M. Mammadov, N. N. Niftiyev, F. I. Mammadov, Synthesis and crystal structure of the FeGaInS<sub>4</sub> compound, *Azerbaijan Chemical Journal*, (2017), 2, 56–59
- <sup>17</sup> F. M. Mammadov, N. N. O. Niftiyev, Dielectric properties of layered FeGaInS<sub>4</sub> single crystals in an alternating electric field, *Semiconductors*, 50 (2016), 1203–1207, doi:10.1134/S1063782616090165
- <sup>18</sup> F. M. Mammadov, et al., Solid-phase equilibria in the FeS–Ga<sub>2</sub>S<sub>3</sub>–In<sub>2</sub>S<sub>3</sub> system and crystal structure of the FeGaInS<sub>4</sub>, in: *Химия твердого тела и функциональные материалы. Термодинамика и материаловедение*, (2018), 362–362
- <sup>19</sup> N. N. Niftiev, et al., Electrical properties of layered FeGaInS<sub>4</sub> single crystals with an alternating current, *Semiconductors*, 43 (2009), 1407–1409, doi:10.1134/S1063782609110025
- <sup>20</sup> F. M. Mammadov, et al., FeS–Ga<sub>2</sub>S<sub>3</sub>–In<sub>2</sub>S<sub>3</sub> system, *Russian Journal of Inorganic Chemistry*, 66 (2021), 1533–1543, doi:10.1134/S0036023621100090
- <sup>21</sup> F. M. Mammadov, et al., Phase diagrams of the FeGa<sub>2</sub>S<sub>4</sub>–FeIn<sub>2</sub>S<sub>4</sub> and FeS–FeGaInS<sub>4</sub> systems, *Kimya Problemleri*, (2019), 1, 58–65
- <sup>22</sup> Z. Addayeva, et al., Fabrication and dielectric spectroscopy analysis of FeGaInS<sub>4</sub>/PVA composite materials, *Journal of Vinyl and Additive Technology*, doi:10.1002/vnl.22148
- <sup>23</sup> X. Hong, L. Zou, J. Zhao, C. Li, L. Cong, Dry-wet spinning of PVA fiber with high strength and high Young's modulus, in: *IOP Conference Series: Materials Science and Engineering*, 439 (2018) 4, 042011, doi:10.1088/1757-899X/439/4/042011
- <sup>24</sup> M. Muradov, et al., Influence of gamma radiation on structure, morphology, and optical properties of GO and GO/PVA nanocomposite, *Radiation Physics and Chemistry*, 208 (2023), 110926, doi:10.1016/j.radphyschem.2023.110926
- <sup>25</sup> M. B. Baghirov, et al., Features of structure and optical properties of GO and a GO/PVA composite subjected to gamma irradiation, *RSC Advances*, 13 (2023), 50, 35648–35658, doi:10.1039/D3RA07186C
- <sup>26</sup> N. Mott, E. Davis, *Electronic Processes in Non-Crystalline Substances*, vol. 2, Oxford University Press, 1982
- <sup>27</sup> A. A. Kononov, N. Y. Nikonorova, R. A. Castro, Characteristic features of the charge transfer processes in the nanocomposites based on polyphenylene oxide with fullerene and endofullerene, *Physics of the Solid State*, 63 (2021), 11, 1670–1674, doi:10.1134/S1063783421100152
- <sup>28</sup> S. R. Elliot, AC conduction in amorphous chalcogenide and pnictide semiconductors, *Advances in Physics*, 36 (1987), 2, 135–217, doi:10.1080/00018738700101971
- <sup>29</sup> M. Muradov, et al., Dielectric properties of PVA/FeGaInS<sub>4</sub> composites: effects of temperature and concentration of fillers, *Journal of Materials Science*, (2025), 1–4, doi:10.1007/s10853-024-10591-x